Recent Progress in Fast-Ion Physics on JET

V.G. Kiptily,[1] S.D. Pinches,[1] S.E. Sharapov,[1] D. Borba,[2] F.E. Cecil,[3] D. Darrow,[4]
V. Goloborod'ko,[5,6] T. Craciunescu,[7] T. Johnson,[8] F. Nabais,[2] C. P. Perez von Thun,[9]
M. Reich,[9] A. Salmi,[10] V. Yavorskij,[5,6] M. Cecconello,[11] G. Gorini,[12] P. Lomas,[1] A. Murari,[13]
V. Parail,[1] S. Popovichev,[1] G. Saibene,[14] R. Sartori,[14] D.B. Syme,[1] M. Tardocchi,[12]
P. de Vries,[1] V.L. Zoita[7] and JET -EFDA contributors[*]

JET-EFDA, Culham Science Centre, OX14 3DB, Abingdon, UK
[1] Euratom / UKAEA Fusion Association, Culham Science Centre, Abingdon, United Kingdom
[2] Euratom/IST Fusion Association, Instituto de Plasmas e Fusão Nuclear, Portugal
[3] Colorado School of Mines, 1500 Illinois Street, Golden, Colorado, USA
[4] Princeton Plasma Physics Laboratory, New Jersey, USA
[5] Euratom/OEAW Association, Institute for Theoretical Physics, University of Innsbruck, Austria
[6] Institute for Nuclear Research, Kiev, Ukraine
[7] Euratom-MedC Association, National Institute for Laser, Plasma and Radiation Physics, Romania
[8] Association EURATOM –VR, Royal Institute of Technology KTH, Stockholm, Sweden
[9] Euratom / MPI für Plasmaphysik Association, Garching, Germany
[10] Helsinki University of Technology, Association EURATOM-Tekes, Finland
[11] Association EURATOM-VR, Division of Applied Nuclear Physics, Uppsala University, Sweden
[12] Associazione EURATOM-ENEA sulla Fusione, IFP Milano, Italy
[13] Consorzio RFX - Associazione Euratom-Enea sulla Fusione, Italy
[14] EFDA Close Support Unit, Garching, Germany

e-mail contact of main author: vasili.kiptily@jet.uk

Abstract. This paper presents recent results on fast-ion studies in JET. The unique diagnostic set for confined and lost particle studies was utilised to investigate the response of fast ions to MHD modes and toroidal field (TF) ripple, and of fast ^{3}He-ions behaviour in shear-reversed plasmas. A dependence of the loss intensity vs. the MHD mode amplitude was derived from the experiments. A study of various plasma scenarios has shown that a significant redistribution of the fast ions happens during the change in the profile of the safety factor from strongly shear-reversed to monotonic. It was found that significant changes in the losses of ICRH accelerated protons are associated with confinement transitions in plasmas. After an L-H transition, an abrupt decrease in the ICRH proton losses was observed. In plasmas with an internal transport barrier, the loss of ICRH-accelerated ions increases as the barrier forms. Further results concerning fast ion losses were obtained during JET experiments in which the magnitude of the TF ripple was varied. The ripple losses of fusion products in high triangularity plasmas appear similar to classical losses, and are in agreement with modelling.

1. Introduction

Future burning plasma devices such as ITER can only tolerate very low levels of fast ion classical and anomalous losses [1]. Even a re-distribution of fast ions is of serious concern for its effect upon the plasma heating profile. In the ITER burning plasma there will be several different groups of fast ions: α-particles and other fusion products, deuterium NBI in the MeV range and ICRH-accelerated ions. It is therefore important to measure and separate the temporal and spatial evolution of these quite different fast ion populations. JET is exceptionally well equipped for such studies since it is capable of simultaneously measuring different species of confined fast ions using its γ-ray diagnostics, and has recently been equipped with new lost ion diagnostics: a thin foil Faraday Cup (FC) array and a Scintillator Probe (SP).

Gamma-rays are emitted in JET plasmas due to nuclear reactions between fast ions and thermal plasma and Be and C impurities [2]. The γ-ray energy spectra uniquely identify the presence of a particular type of fast ions, and such spectra are measured on JET with three

---

[*] See the Appendix of F. Romanelli et al., paper OV/1-2, this conference

independent devices [2], one with a quasi-tangential, and two with vertical lines of sight, through the plasma centre. The γ-ray spectra are continuously recorded during all JET discharges over the energy range 1-28 MeV. For identification of the fast ions, which exist in the plasma and produce the observed γ-ray emission, and in order to assess the effective tail temperatures of these fast ions, the γ-ray spectrum modelling code, GAMMOD [2] is used. In addition the GAMMOD analysis gives the fast ion density and the contribution to the neutron yield from the fast particle-induced reactions.

Spatial profiles of the γ-ray emission in the energy range $E_\gamma >1$ MeV are tomographically reconstructed on JET by using the γ-cameras, which have ten horizontal and nine vertical collimated lines of sight [3]. The data acquisition system accommodates the line-integrated γ-ray count-rate measurements in up to 4 independently adjustable energy windows. Each window is set to correspond to the γ-ray peak(s) from a given fast ion population, thus different groups of fast ions emitting γ-rays of different energies are simultaneously measured with the same γ-camera.

In addition to the diagnostics of confined fast ions, the newly installed Faraday Cup array [4] detects lost fast ions at multiple poloidal locations. The array consists of nine detectors spread over five poloidal locations below the mid-plane just outside the plasma. Along the major radius, the detectors are equally spaced in three locations. The detection of the temporal evolution of the fast ion current signals in the radially and poloidally distributed detectors provides a map of lost particle fluxes at different locations with time resolution of about 1 ms.

Another newly installed lost ion diagnostic detector, the scintillator probe (SP) [5] allows the detection of lost ions at a single position outside the plasma, and provides information on the lost ion pitch angle between 30° and 85° (5% resolution) and its gyro-radius between 30 and 140 mm (15% resolution) with a time resolution of 10 ms. The scintillator probe is located just below the mid-plane. The underlying principle of scintillator measurements is the emission of light by a scintillating material after a fast particle strikes this material. Selection criteria for the particles that hit the scintillator are introduced by using a set of collimators matched to the equilibrium magnetic field of JET. An optical arrangement within the scintillator probe is used to transfer the light emitted by the scintillator towards a charge-coupled device CCD camera and a photomultiplier array through a coherent fibre bundle.
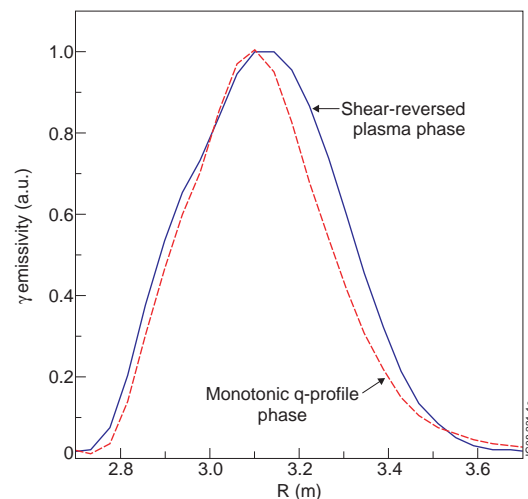

FIG.1. Mid-plane profiles of γ-ray emissivity obtained by tomographic reconstruction of the 2D γ-camera data of the ^{3}He-minority ICRH discharge #69436 (I_P=2.3MA, B_T =3.1T): blue - shear-reversed plasma phase, t=5.25s; red - monotonic q-profile phase, t=6.75s.

2. Measurements of spatial redistribution of confined fast ions in D-^{3}He fusion plasmas

In order to test the ability of JET fast ion diagnostics to detect spatial re-distribution of confined fast ions due to equilibrium changes and due to excitation of MHD modes (fishbones, toroidal Alfvén eigenmodes and Alfvén cascades) driven by RF heated fast particle populations, measurements of ^{3}He-minority ICRF accelerated ions were performed using the γ-ray diagnostics. Previously reported studies on JET [6] have demonstrated that ICRH acceleration of ^{3}He minority ions in deuterium plasmas provides a significant rate of D-

^{3}He fusion. Hence this scenario may be used for investigating highly energetic 3.6 MeV alpha-particles and 15 MeV protons born in these fusion reactions, without activating the machine as in deuterium-tritium plasma experiments. Nuclear reactions with the main impurities, ^{12}C(^{3}He,pγ)^{14}N, ^{9}Be(^{3}He,nγ)^{11}C, ^{9}Be(^{3}He,pγ)^{11}B gave rise to intense γ-ray emission, which may be used for the fast ^{3}He-ion studies ($E_{3He} > 0.9$ MeV). Gamma-ray spectra show that the energetic ^{3}He-tail with an effective temperature 200-450 keV was driven by ICRF heating in these discharges.

First, it was found that a significant change in the spatial profile of the gamma-rays from the fast ^3He ions occurs when the profile of the safety factor (q) changes from strongly shear-reversed to monotonic. Fig.1 shows two γ-ray emission profiles in the mid-plane, obtained during ^{3}He-minority heating in the same JET discharge, in which a monotonic q-profile was evolving into a shear-reversed q-profile so that Alfvén cascades were observed [7]. Gamma-ray images of energetic ^3He-ions were recorded with 2-D γ-ray cameras. The figure demonstrates that the MeV ^{3}He-ion profile in the non-monotonic phase of the discharge is ~ 25% broader than the profile in the monotonic phase due to the change of the orbit topology.

Second, evidence of MeV ^{3}He-ion redistribution during sawtooth crashes has been also obtained with the 2-D γ-ray camera. The

FIG.2. Tomographic reconstructions of γ-ray emission profiles obtained with the 2D γ-camera [3] in the ^{3}He-minority ICRH discharge #69429 (I_P=3MA, B_T =3.1T): left – before a sawtooth crash; right – after the crash; bottom – magnetic spectrogram.

upper two figures in Fig.2 show the tomographic reconstructions of the γ-ray emission produced by ^{3}He-ions in ^{12}C+^{3}He, ^{9}Be+^{3}He nuclear reactions. The left profile was recorded during a fishbone preceding a sawtooth crash; the right one was after the sawtooth crash (see magnetic spectrogram in Fig.2, bottom).
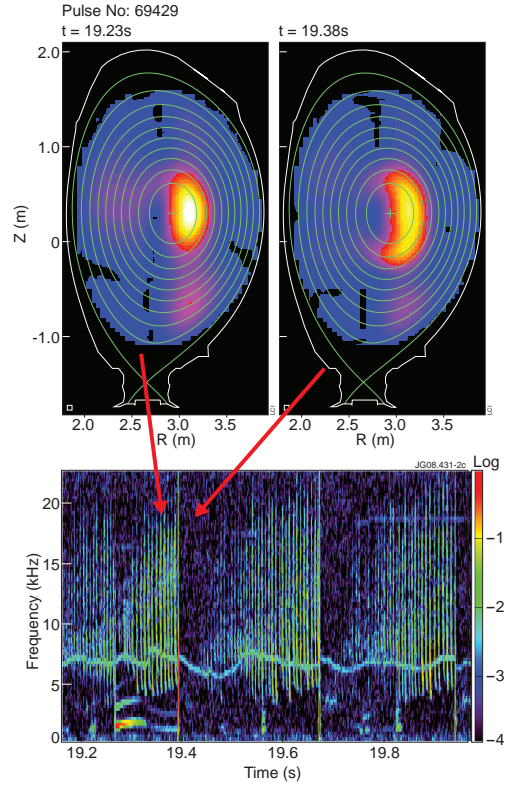
3. Fast ion losses induced by Toroidal Alfvén Eigenmodes and Alfvén Cascades

The measured 17-MeV γ-rays of the D(^{3}He,γ)^{5}Li reaction indicate the rate of the D(^{3}He,p)^{4}He fusion reaction, which produces α-particles at 3.6 MeV and protons at 15 MeV and in most of the discharges this rate was rather high. During these discharges, the fast-ion loss scintillator probe shows that the fusion α-particles more intensively escape from the plasma during Alfvén cascade and tornado mode activity [8]. It is expected that losses of 15 MeV fusion protons, having Larmor radii outside the SP measurement range of 140 mm, take place as well. There are two possible reasons for the observed effect of the loss dependence on the Alfvénic activity. First, ICRH-accelerated ^{3}He ions with tail temperature of few hundred keV, which are the source for D(^{3}He,p)^{4}He fusion reaction, may be so strongly re-distributed by a resonant interaction with the Alfvénic modes, that the re-distribution of ^{3}He affects the profiles of α-particles born in D(^{3}He,p)^{4}He fusion reactions. Second, the perturbed magnetic field associated with the Alfvénic modes, may directly affect the fusion-born α-particles in the region of the phase-space close to the boundary between confined an unconfined particles.

Dedicated discharges with ^{3}He ICRF minority heating (no NBI) in deuterium plasmas were run to study the influence of Alfvénic MHD, Toroidal Alfvén Eigenmodes (TAEs) and Alfvén Cascades (ACs) on fast ion losses. In the MHD-free reference discharges two types of losses were observed on the scintillator plate – denoted here as type **A** and type **B** (Fig.3a). From orbit reconstructions (Fig.3b) it is found that the detected type **A** losses correspond to trapped particles whose banana tips are close to the RF resonance layer at intermediate minor radii. It is also found that the temporal evolution of the light emission for the type **A** losses follows the 17 MeV γ-ray emission (D-^{3}He fusion rate indicator) from the γ-ray detectors. From this and the observed range of lost particle energies, which turn out to be consistent with kinematical calculations, the type **A** losses are identified as alpha particles on banana orbits, which are born from D-^{3}He reactions near the ICRF resonance layer and then lost promptly. The red symbols in Fig.3c show the light yield for type **A** losses for the MHD-free reference discharges. It can be seen that the light yield increases linearly with the achieved D-^{3}He fusion yield. It is noted that the particles responsible for the type **B** losses are born closer to the plasma centre, and that their identity is still under investigation. A likely candidate are protons born from reactions of ^{3}He with impurities (Be and/or C).
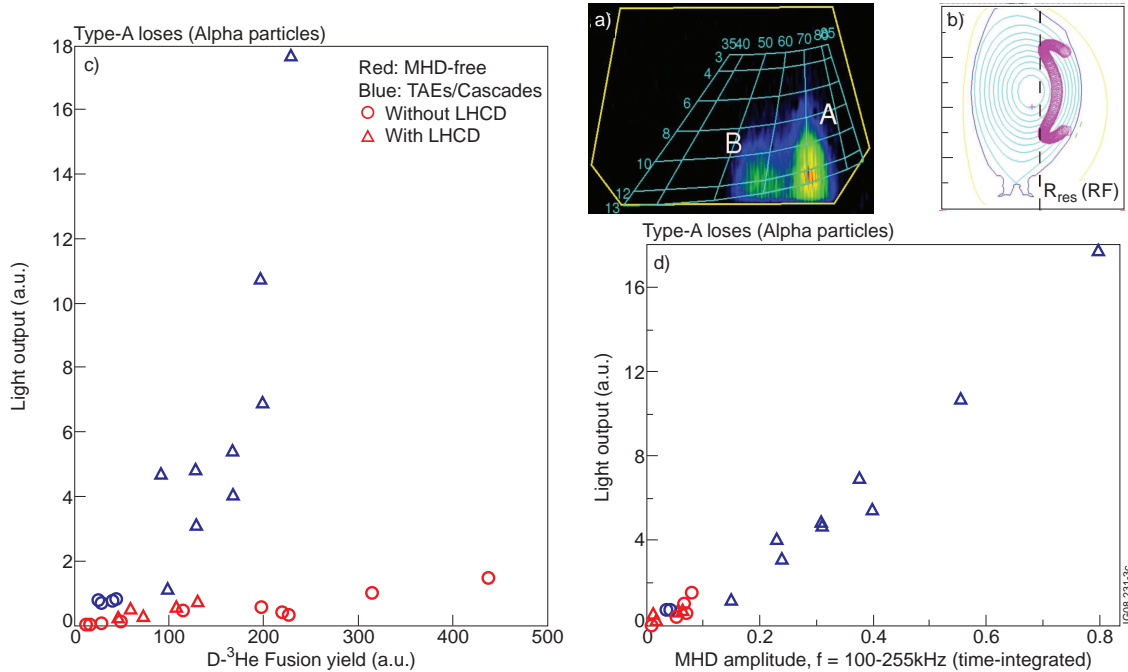

FIG.3. a) Loss spots observed on the scintillator plate; b) ORBIT code reconstructions for detected losses of type A; c) light output on the scintillator plate for losses of type A (the light emission is integrated over the relevant spot area of the CCD chip for each time frame, and then time-integrated) versus D-^{3}He fusion yield (from BGO gamma ray detector; d) same loss data as in c), but plotted against the amplitude of the Alfvénic MHD (see text).

In the presence of TAEs/Cascades, a linear scaling of type **A** losses on the D-^{3}He fusion yield does not apply (Fig.3c, blue symbols). For a given *D-^{3}He* fusion yield, the type **A** light yield increases by a factor that ranges from 2 to 40. Hence, not only can the factor be very high but it also varies considerably. To quantify the losses on the intensity of Alfvénic perturbations that has been excited, the following method has been applied: a digital band-pass filter is applied to a signal from a magnetic pick-up coil through a time-windowed FFT and selection of the desired frequencies (in this case 100-255 kHz). Before back-transforming, the amplitude at each frequency ω is divided by ω to account for the increasing sensitivity of pick-up coils with frequency. Finally, the resulting envelope for that signal is integrated over the relevant time-interval. Figure 3d shows the same loss data as in Fig.3c, plotted against the obtained MHD amplitude. This yields the important conclusion that the MHD-induced α-

losses amplification is directly determined by the MHD amplitude, on which it depends linearly [9]. This linear dependence indicates that the increase of lost particles is most likely to be associated with the effect of Alfvénic perturbations on the boundary between confined and unconfined particles in phase space [10].

4. MHD-induced resonant loss

Alfvénic instabilities causing resonant fast ion redistribution and losses were found in a sawtoothing H-minority ICRH plasma with a safety factor profile $q(0)<1$ [8, 11, 12]. The temporal evolution of fast ion losses with resolution on energy and pitch angle was measured using the new SP, which allowed the determination of the orbits of fast ions that reached the detector. The fast ions in resonance with the different instabilities present in the plasma were identified using the CASTOR-K code [13]. It was then possible to identify which instabilities were responsible for the losses collected in the detector. Two different phases of losses, with different characteristics, were identified. The first phase occurs after a sawtooth crash (Fig.4, upper), when TAE and high frequency fishbones are unstable. In this phase, TAE are responsible for most of the measured losses. Losses caused by precessional drift fishbones, if any, are not significant. The second phase initiates when the core-localized TAE modes, so-called "tornado modes" become unstable: the intensity of losses increases by a factor from 2 to 5, the average energy of the ions that reach the detector decreases and its pitch angle increases (Fig.4, lower). In this phase, the losses are mostly triggered by resonant interaction with the tornado modes. When fast ions interact with tornado modes, they are transported from the plasma core to a more peripheral region of the plasma while their orbits suffer a topological transition from potato to banana orbits. In this region, tornado and TAE eigenfunctions overlap and the fast ions will start interacting with TAE, which have around the same frequency and same toroidal n number as tornado modes. TAE will eventually end up by expelling these fast ions from the plasma [11, 12].
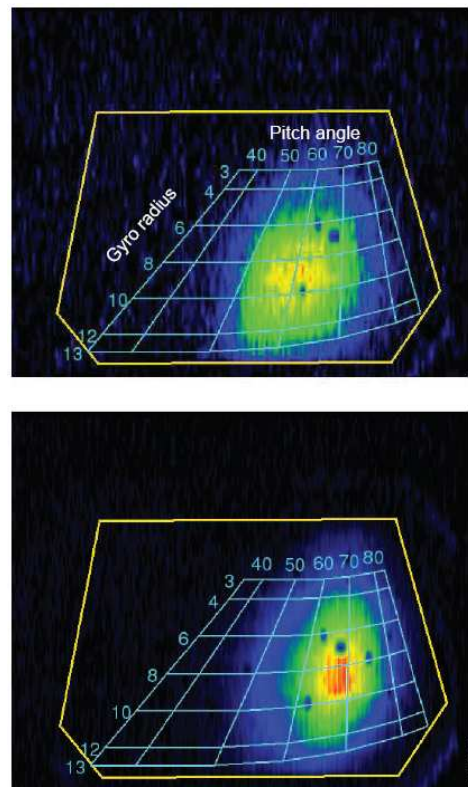

FIG.4. JET discharge #66380, I_P=2.5MA, B_T=2.7T Footprints of fast protons lost at the SP during periods when: TAE and precessional fishbones are unstable (upper); tornado and TAE modes are unstable (bottom).

5. Fast-ion loss in sawtooth crash

The dynamics of the fast ion losses was studied in the H-minority ICRH scheme as well. Figure 5 shows the temporal evolution of pitch-angles and gyro-radii of lost ions measured with SP during a sawtooth crash. Gamma-ray spectrometry indicates the presence of fast protons and deuterons accelerated with 2nd harmonic ICRF heating in this discharge. It is seen that before the crash, losses of ions with very large Larmor radii, >12 cm, and in a narrow pitch-angle, are dominant. These lost ions are identified as ICRH-accelerated protons. During the crash, the majority of the lost ions identified as deuterons have a much lower energy and are close to the trapped-passing boundary. After the crash, both types of losses co-exist for some time before a relaxation to the initial pre-crash state is observed. The ICRH minority heating scheme generates particles which can be classified by their pitch angle outside the

5

plasma (e.g. at SP). The HAGIS code [14] has been used to identify the part of the fast ion distribution function that is expelled from the plasma in relation with the destabilisation of sawteeth. The orbits of sawtooth related fast ion losses are found to originate near the sawtooth inversion radius for 2 exemplary cases. Strong additional losses are confirmed to originate from the $q=1.5$ surface at the same time when a $m=3$, $n=2$ tearing mode is excited which was seeded by the sawtooth crash. Fishbone and sawtooth instabilities were seen to redistribute particles onto loss orbits from within and outside the sawtooth inversion radius, respectively [15].
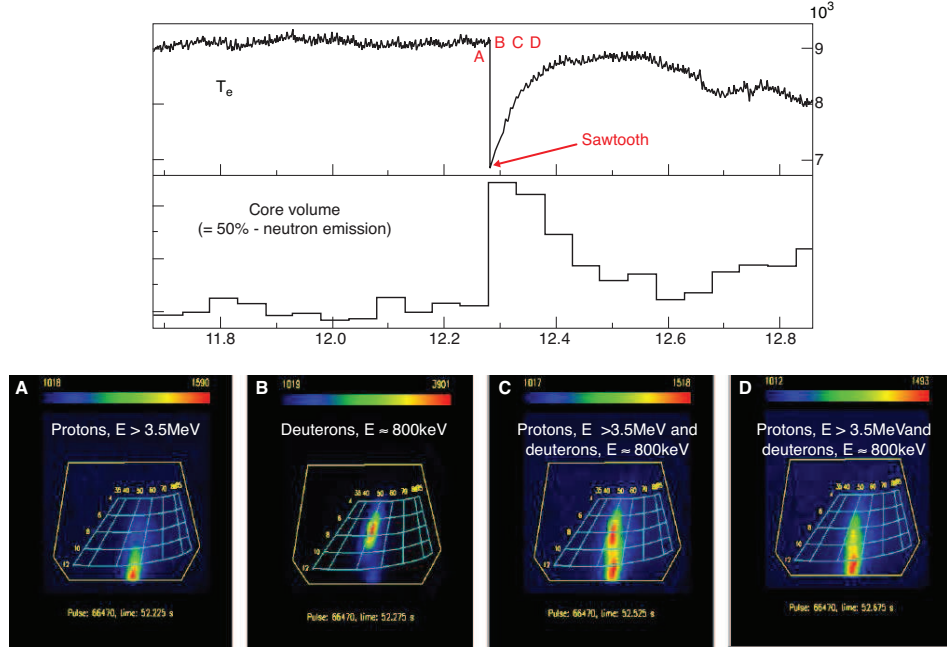

FIG.5. JET pulse #66470, I_P=2.5MA, B_T=3T. Top: central electon temperature vs. time; middle: plasma core volume changes during the sawtooth crash period; bottom: footprints of fast protons/ deuterons lost in SP during sawtooth periods A(12.225s), B(12.275s), C(12.575s) and D(12.675s).

6. Fast-ion losses during L-H transition and ITB formation

A significant change in fast ion losses has been detected during L-H transition in JET plasmas with combined NBI and H-minority ICRF heating. Gamma-ray diagnostics indicated that both fast protons and deuterons accelerated with 2nd harmonic ICRF heating are present in the plasmas. Two types of losses were observed on the scintillator plate which was identified as first orbit (FO) losses of fusion products (Fig.6, blue) and losses of ICRF accelerated ions (Fig.6, red). Significant changes in the losses of ICRH accelerated protons and deuterons happen after the confinement transition (L-H transition) as Figure 6 shows.

Another essential effect of plasma confinement regime on the fast ion losses has been found in the Advanced Tokamak (AT) scenario discharges. In plasmas with an internal transport barrier (ITB), the loss of ICRF accelerated ions increases by an order of magnitude (Fig.7, red) as the barrier forms. During both the L-H transitions and ITB formation (t~5s), no anomaly in the expected FO loss rate of fusion products (Fig.7, black) is observed (it follows the neutron rate, Fig.7, blue), in contrast to that for the ICRF accelerated ions. The very significant difference between the losses of fusion products (which don't change) and the losses of ICRF accelerated fast ions (which change significantly) remains to be explained. It is likely that the large difference in the fast ion energy between the species mentioned above makes a strong impact on the efficiency of fast ion interaction with turbulence associated with

6

the confinement transitions, such as the experimentally observed magnetic turbulence in the range up to 250 kHz on JET [16].
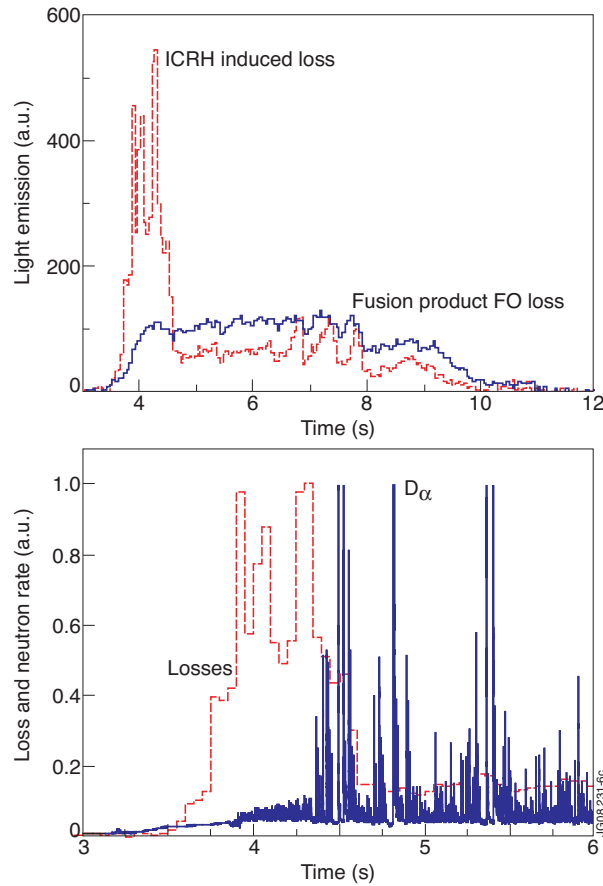

FIG.6. H-mode discharge: top - time traces of light emission at SP, related to ICRF-induced and FO fusion-product losses; bottom - ICRF-induced losses and D_α-emission.

7. Fusion product losses in the ripple experiments

In JET, which has a set of 32 coils, the toroidal magnetic field (TF) ripple is rather small, $\delta \approx 0.08\%$ at the separatrix. However, JET TF can be configured to run different currents in odd & even numbered coils, to increase TF ripple at the plasma boundary up to $\delta \approx 3.0\%$ to give a much close representation of ITER ripple. Here, results of observations of the fusion products (p, T) losses induced by an N=16 TF ripple harmonic are presented. In a series of experiments [17], the TF ripple was varied from the standard JET TF ripple, 0.08%, to an intermediate high level of 1.0% at around $B_T(0) = 2.2$ T.

The fusion product losses were measured with the SP. The ripple effects on fusion product losses in low (LT) and high triangularity (HT) H-mode plasmas were observed. There is evidence of MeV-ion redistribution due to the ripple. Modelling of 3 MeV fusion reaction protons has been done with a guiding centre following Monte Carlo code ASCOT [18]. Protons have been sampled from an experimentally reconstructed 2-D fusion reactivity distribution and followed in an EFIT

magnetic equilibrium together with toroidal magnetic field ripple and collisions. Collected guiding centre distribution has been corrected with the device transmission function to get the final SP response. A comparison of pitch-angle loss profiles for the 3-MeV fusion protons measured in the HT H-mode discharges with normal and 1% TF ripples are presented in Fig.8 (upper). The modelling results placed below are qualitatively consistent with the experimental data that demonstrate a ripple effect on the fusion product first orbit losses. In the modelling it was observed that the extra protons measured by SP at high pitch angles in the case of 1% ripple operation were due to collisionless stochastic ripple banana diffusion pushing the protons born
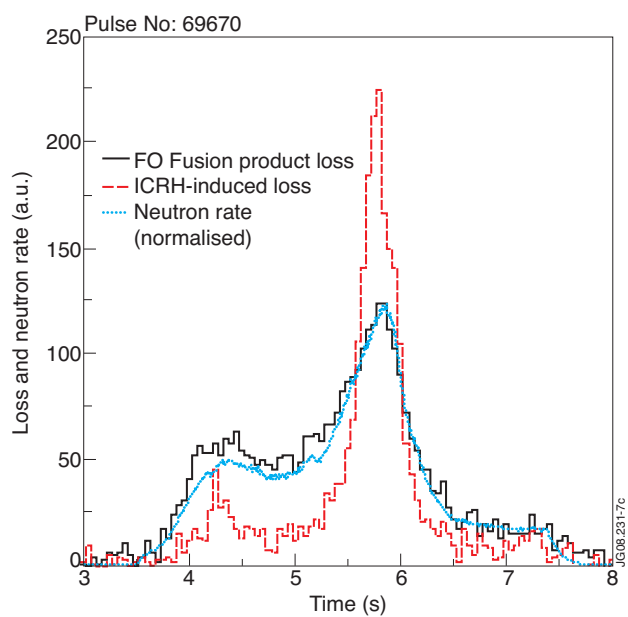

FIG.7. Time traces of light emission at SP, related to ICRF-induced and FO fusion-product losses and neutron rate in the discharge with ITB.

with low parallel velocity in the strong ripple region into the loss cone. Note, however, that the modelled pitch-angle distribution of ripple losses is quantitatively different from the measured one.
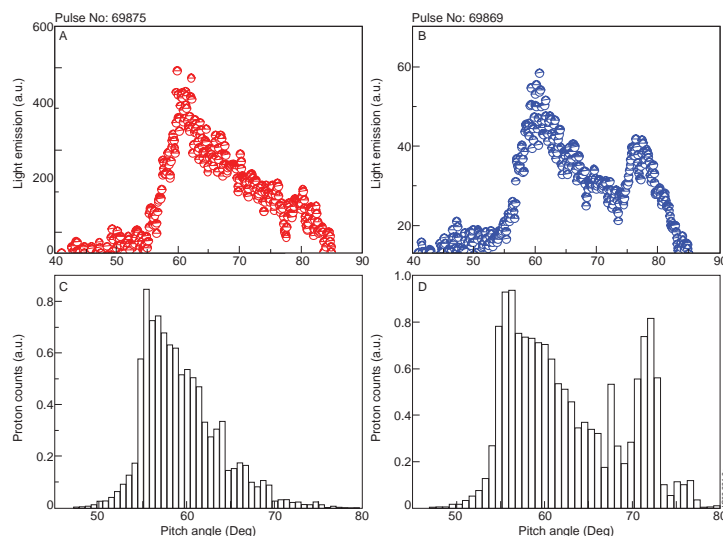

FIG.8. Top: pitch-angle distributions of fusion product losses relevant to 13-cm gyro-radius, detected by SP during high triangularity H-mode plasmas, and related to **A** – discharge with a normal TF ripple, 0.08%; **B** – discharge with 1% ripple. Bottom: **C** and **D** – results of the ASCOT modelling for the cases 0.08% (JET discharge #69875) and 1%, (JET discharge #69869) respectively.

8. Summary

An account of recent JET results on fast-ion studies with a unique diagnostic set has been presented. A linear dependence of the loss intensity vs. the MHD mode amplitude has been directly derived from the experiments. It is shown that a significant redistribution of the fast ions happens during the change in the q-profile. It was found that essential loss changes are associated with confinement transitions (L-H transition, ITB) in plasmas. In the ripple experiments, losses of fusion products were determined to be in qualitative agreement with classical loss mechanisms.

References

[1]. FASOLI, A., et al., Nuclear Fusion **47** (2007) S264–S284.
[2]. KIPTILY, V.G., et al., Nuclear Fusion **42** (2002) 999.
[3]. KIPTILY, V.G., et al., Nuclear Fusion **45** (2005) L21.
[4]. DARROW, D. S., et al., Rev. Sci. Instrum. **75** (2004) 3566.
[5]. BAUMEL, S., et al., Rev. Sci. Instrum. **75** (2004) 3563.
[6]. JACQUINOT, J. and SADLER, G.J., Fusion Technology **21** (1992) 2254.
[7]. SHARAPOV, S.E., et al., Nuclear Fusion **45** (2005) 1168.
[8]. SANDQUIST, P., et al., Physics of Plasmas **14** (2007) 122506.
[9]. PEREZ VON THUN, C. P., et al., to be submitted to Physical Review Letters.
[10]. WHITE, R.B. and CHANCE, M.S., Phys. Fluids **27** (1984) 2455.
[11]. NABAIS, F., et al., 34 EPS Conf. on Plasma Phys., Warsaw, July 2-6, 2007, P-1.123.
[12]. NABAIS, F., et al., to be submitted to Nuclear Fusion.
[13]. BORBA, D. and KERNER, W., J. Computational Physics **153**, 101 (1999).
[14]. PINCHES, S. D., et al, Comp. Phys. Comm. **111**, 131 (1998).
[15]. REICH, M., et al., 34 EPS Conf. on Plasma Phys., Warsaw, July 2-6, 2007, O-4.016.
[16]. SHARAPOV, S.E., POLI, F.M., to be submitted to Nuclear Fusion.
[17]. SAIBENE, G., et al., 34 EPS Conf. on Plasma Phys., Warsaw, July 2-6, 2007, O-4.001.
[18]. HEIKKINEN, J.A., SIPILÄ, S.K., Phys. Plasmas **2** (1995) 3724.